Organic–Inorganic Behavior of Plasma-Polymerized Hexamethyldisiloxane Films Studied by Electron and Photon Induced Ion Desorption

ARTICLE *in* PLASMA PROCESSES AND POLYMERS · JULY 2013

Impact Factor: 2.45 · DOI: 10.1002/ppap.201300007

Organic–Inorganic Behavior of Plasma-Polymerized Hexamethyldisiloxane Films Studied by Electron and Photon Induced Ion Desorption

Amanda G. Veiga, Yunier Garcia-Basabe,* Ralph Schmittgens,[a] Maria Luiza M. Rocco*

In the present work two thin films, fabricated by plasma-polymerization of hexamethyldisiloxane (HMDSO) monomer, were studied by a combination of electron (ESID) and photon (PSID) stimulated ion desorption techniques. The organic character of the polymer film is evidenced by the high contribution of $C_2H_n^+$ species and the absence of high mass fragments in its ESID spectrum. On the other hand, the inorganic character is elucidated by the presence of high mass silicon ionic fragments. NEXAFS and PSID spectra also show clear differences between organic and inorganic films. The marked reduction of CH_3^+ species for PSID spectra of the organic–polymeric film is in accordance with ESID analysis and may be interpreted by a screening effect of its cross-linked organic structure.

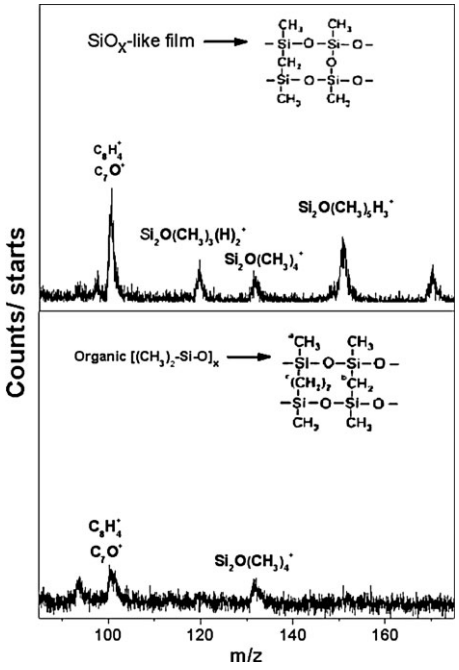

1. Introduction

In recent years, plasma-polymerized thin films containing siloxane have attracted increasing interest for applications in several fields as optics, electronics, sensors, coatings, and biomedicine. The relevant properties of these films can be modified widely by a suitable choice of source monomer and deposition parameters. Furthermore, various silicon monomers are sufficiently volatile, non-toxicant, non-flammable, and relatively cheap, so it becomes the more secure and less expensive process.[1–4]

In this context, the organosilicon plasma polymers obtained from hexamethyldisiloxane (HMDSO) monomer has received considerable attention due to the ease and safety in handling.[5] There are extensive reports in the

A. G. Veiga, Y. Garcia-Basabe, M. L. M. Rocco
Instituto de Química, Universidade Federal do Rio de Janeiro, Cidade Universitária, Ilha do Fundão, 21941-909, Rio de Janeiro, RJ, Brazil
Fax: +55 21 2562 7265;
E-mail: yunier@iq.ufrj.br, luiza@iq.ufrj.br
Y. Garcia-Basabe
Department of Physics, Faculty of Engineering, University of Matanzas "Camilo Cienfuegos", Matanzas 40100, Cuba
R. Schmittgens
Institut für Festkörperelektronik, TU Dresden, 01062 Dresden, Germany
[a]Current address: Leica Camera AG, Oskar-Barnack-Str. 11, 35606 Solms, Germany.

Plasma Process. Polym. **2013**, DOI: 10.1002/ppap.201300007

DOI: 10.1002/ppap.201300007

literature about the chemistry structure of HMDSO plasma deposited films.[6–14] Among these studies, several highlight the relation between plasma polymerization conditions (pressure, power, flow rate, current density, operation mode, carrier gases content, etc) and the chemical behavior of the film. By varying these process parameters thin films with different chemical composition and structure can be obtained from the monomer.[9,12,13,15] For example, it is known that from radio-frequency (RF) and microwave plasma experiments plasma-polymers deposited in a HMDSO-oxygen plasma can be varied from a soft, siloxane-like polymer structure to a hard, amorphous silicon oxide film.[9,10,13,16]

In this framework, studies on the interaction of electrons and photons with plasma-polymerized thin films are very important for surface morphology and composition investigations because with the understanding of the chemical structure and electron- and photo-fragmentation mechanisms it is possible to determine their potential uses in new applications. Although its importance, very few results can be found.

There are some reports on the interaction of the HMDSO molecule with low energy electrons (energy 70 eV).[14,17–19] Basner et al.[17] presented electron impact ionization studies on HMDSO and found that $Si_2O(CH_3)_5^+$ species are the most abundant ionic fragment in the mass spectra. On the other hand, Carles et al.,[19] reported the dissociative recombination of electrons in HMDSO cation as well as the ion molecular reaction between Ar^+ and HMDSO using mass spectrometry. Jauberteau and Jauberteau[14] investigated the interaction of the HMDSO molecule with low energy electrons (15–70 eV energy range), with Ar ($^3P_2$) metastable species (11.55 eV internal energy) and with VUV photons (7.3–10.79 eV). In each case different dissociation mechanisms were found induced by Si–C or Si–O bond breaking.

Ionic fragmentation induced by high energy electron (ESID) or photon (PSID) impact is well explained by the Auger process (Auger stimulated ion desorption, ASID), the decay process to follow an excited core hole, which predominates for light elements. The formations of positive holes in localized valence orbitals may lead to fragmentation around the exciting atom, with subsequent desorption. The use of tunable synchrotron radiation allows the controlling of chemical reactions on surfaces, which can be followed by PSID coupled to core-level excitation. Different elements can be probed and chemical shifts explored. Another important process, leading also to fragmentation and desorption of ionic species, is due to energetic Auger electrons, photoelectrons, and secondary electrons, most of them originated in the bulk, the so-called XESD (X-ray induced electron stimulated desorption) process.[20–24]

In this work, two plasma-deposited HMDSO films previously synthetized and characterized by conventional techniques (FTIR, electron microscopy, and AFM) [12,13] have been studied combining the electron (ESID) and photon (PSID) stimulated ion desorption methods. The aim of our investigation is to show the potentiality of the ion desorption techniques for identifying the organic–inorganic character of these two plasma deposited films.

2. Experimental Section

The polymer films studied in this work were prepared using a plasma polymerization procedure described in detail elsewhere.[12,13] Two samples were synthesized using the experimental parameters presented in Table 1, which will be referred to hereafter as HDMSO_1 and HDMSO_2. The films were deposited on Si(110) monocrystalline substrate previously purified in the deposition chamber by argon plasma treatment.

ESID experiments were carried out using an experimental set-up implemented in our laboratory that consist in a sample manipulator and a time-of-flight mass spectrometer (TOF-MS) housed in an UHV chamber with a base pressure of about 10^{-9} mbar. The homemade TOF-MS works basically from an electrostatic ion extraction system with collimating electrostatic lens, a drift tube, and a pair of microchannel plate (MCP) detectors, disposed in the chevron configuration. After extraction, positive ions travel through three metallic grids (each of which with a nominal

Table 1. Experimental parameters used in the plasma polymerization procedures.

Experimental parameters	HDMSO_1	HDMSO_2
Vacuum	10^{-5} mbar	10^{-5} mbar
VHF power	150–300 W	150–300 W
Total gas flux	100 sccm	100 sccm
HMDSO/O_2 ratio	1/5	1/5
Total pressure (Ar/HMDSO/O_2)	8 Pa	8 Pa
HMDSO content (% total pressure)	5%	14%
Deposition time	300 s	300 s
Operation mode	Continuous	Pulsed

DOI: 10.1002/ppap.201300007

transmission of 90%), before reaching the MCP. The electric potentials were chosen from an ion optic simulation performed with the SIMION 3D software[25] assuming ions with up to 10 eV initial kinetic energy and initial angular spread from 0 to 90°. The polymer films were irradiated with an electron gun operating in a pulsed mode (80 kHz frequency and 20 ns pulse width). A constant positive electric potential was applied to the sample to extract the ionic species. The final electron beam energy is given by the sum of the nominal energy of the electron gun (variable) and the electric potential applied. Incident electron currents of the order of nanoamperes were used throughout the measurements, which ensure that the electron–sample interaction is an isolated event and prevents sample degradation. The output signal was processed by standard pulse electronics and used to provide a stop signal to the time- to digital-converting (TDC), which has a time resolution of 1 ns per channel.

PSID experiments were performed at the Brazilian Synchrotron Light Source (LNLS), during a single-bunch operation mode of the storage ring with a period of 311 ns and width of 60 ps. The soft X-ray spectroscopy (SXS) beamline, mounted with a double-crystal type monochromator using the InSb(111) plane, gives an energy resolution of ~2.8 eV at 4 keV.[26] The experimental set-up used here is similar to that of ESID experiments. In this case a 1/148 divider was used to take the synchrotron radiation (SR) pulse timing from the 476.066 MHz frequency signal from the microwave cavity of the storage ring, which was used as trigger of the experiment and also used as the start signal for the TDC. The desorbed positive ions were extracted, collimated, and further transmitted through the 25 cm drift tube, before being detected by the MCP. The mass calibration procedure and fragment assignment was performed based on a combination of traditional mass calibration method and ion software simulation.[21,27] The TOF spectrum obtained using the temporal window of 311 ns of the single-bunch mode is calibrated using the following equation: $TOF = [(TOF_{simion}/311) - n] \times 311$, where TOF_{simion} and n represent the simulated time of flight using the SIMION 3D software[25] and the number of cycles that has passed from the desorption of the ion to its detection (number of starts), respectively. Because of this light ionic species can appear at higher time of flight values than heavier ions in the PSID spectra.

Photoabsorption (NEXAFS – near-edge X-ray absorption fine structure) spectra were also recorded by measuring the total electron yield, TEY (drain current at the sample) simultaneously with a photon flux monitor (Au grid) for normalization due to fluctuations in the beam intensity. The energy calibration was performed by taking the well-known value for the L_{III} transition ($2p_{3/2} \rightarrow 4d$) of metallic molybdenum.[28]

3. Results and Discussion

3.1. ESID Analysis

ESID spectra of both samples, HDMSO_1 and HDMSO_2, obtained at different synthesis parameters and using electron beam energy of 2 200 eV, are reported in Figure 1. To improve figure analysis the intensity scale was enlarged and divided into different mass ranges. Similar to other reported ESID analysis of organic compounds[23,29,30] H^+ ion is the main species desorbed after electron bombardment, followed by heavier fragments with lower intensity. Peak assignment of the siloxane fragments in the ESID spectra (Table 2) was performed considering the TOF-SIMS results[31,32] and ESID spectra obtained with low energy electrons (energy ≤70 eV)[4,16,17,33,34] previously reported. F^+ and F^{2+} peaks found in the HDMSO_2 ESID spectrum is probably due to silver paint contribution, used to maintain the electrical contact. Peak corresponding to F^+ at m/z 19 may have contribution from the H_3O^+ ionic species. The latter ion can be originated by monomer fragmentation during plasma polymerization process or by water adsorption from environment. The origin of this species will be discussed in detail later.

From a comparative analysis between the ESID spectra of both samples we can clearly observe the effect of the synthesis parameters in the polymer film structure. The qualitative comparison shows that the two samples present different fragmentation profiles. The principal difference is the presence of low intensity peaks in the high mass region for HDMSO_2 compared to HDMSO_1 sample. For HDMSO_2 it was practically not possible to find species with masses higher than 105 a.m.u. Higher masses species in the HDMSO_1 spectrum were attributed to siloxane connected to methyl groups. Accordingly to the mass spectra comparison we can observe that except for the H^+ peak, the most intense peak in the HDMSO_1 spectrum is at m/z 15 attributed to CH_3^+ species while in HDMSO_2 spectrum this corresponds to m/z 29 attributed to $C_2H_5^+/SiH^+$ species. These results show clearly that the monomer flux and the plasma exposition modes (pulsed and continued) as reported by Schmittgens et al.[12,13] in previous studies can modify the chemical structure of the plasma deposited films. Another support for the organic character of the HDMSO_2 film is the higher contribution of $C_2H_n^+$ fragments in its ionic desorption spectrum as compared to HDMSO_1. The peak intensity reduction of CH_3^+ species in HMDSO_2 can be related with the formation of more complex cross-linked chains in the polymer structure screening the formation of this ion. Due to the organic structure and therefore the high hydrophobicity of the HDMSO_2 polymer we can conclude that the H_3O^+ species found in their ESID spectra are originated during plasma polymerization process and not by the presence of water in the structure of the polymer. On the other hand the presence of OH^+ (16 a.m.u) and $SiOH^+$ (47 a.m.u) in the HMDSO_1 ESID spectrum is strong confirmation of its inorganic character. The last result is in accordance with Morent et al.[15] who report that the presence of Si−OH and OH groups in the FTIR spectra is evidence for an inorganic character in plasma-deposited films. In the case of HMDSO_2 film, where an organic

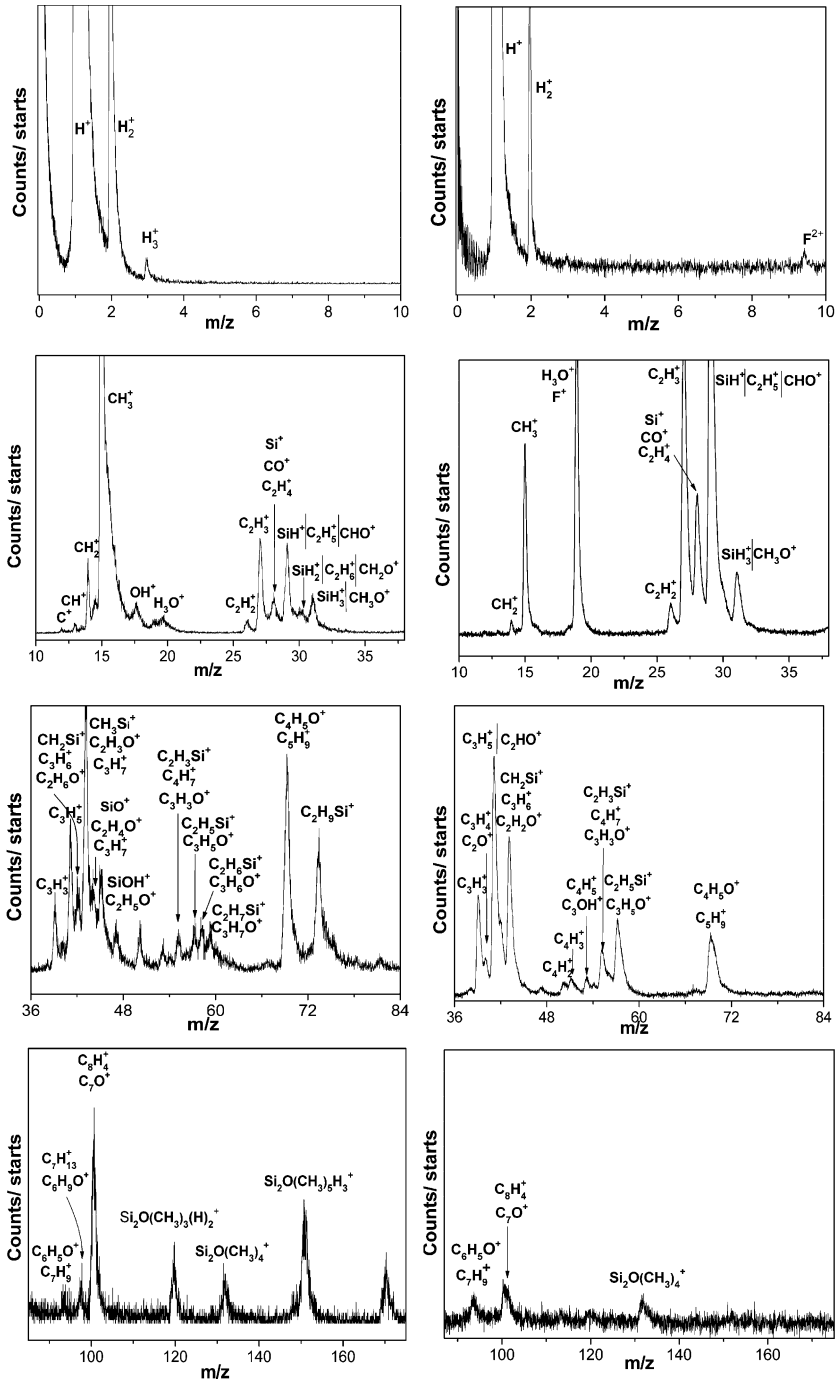

Figure 1. ESID spectra at different mass ranges obtained at 2 200 eV electron beam energy for HDMSO_1 (left) and HDMSO_2 (right) films.

character is predominant, these fragments were not found in its ESID spectrum.

In order to improve our knowledge on the ionic fragmentation mechanism of these polymeric films, we have evaluated desorption ion yields measured as a function of the electron impact energy for HMDSO_1 sample. The evaluation of the relative ion yields was performed dividing the area of a given peak by the start signal. Gaussian fitting was used to determine the peak areas. Figure 2 and 3 shows desorption ion yields as a function of the electron impact energy for the most representative ionic fragments. In the case of $C_mH_n^+$ species showed in Figure 2 we can observe two maxima at energies corresponding to about two-three times the C *K*-edge

Table 2. Mass assignment and suggested fragments measured by ESID-TOF.

m/z	Probable ion fragments	
	HMDSO_1	HMDSO_2
1	H^+	H^+
2	H_2^+	H_2^+
3	H_3^+	–
9	–	F^{2+}
12	C^+	–
13	CH^+	–
14	CH_2^+	CH_2^+
15	CH_3^+	CH_3^+
17	OH^+	–
19	H_3O^+	F^+/H_3O^+
26	$C_2H_2^+$	$C_2H_2^+$
27	$C_2H_3^+$	$C_2H_3^+$
28	$C_2H_4^+\|Si^+\|CO^+$	$C_2H_4^+\|Si^+\|CO^+$
29	$C_2H_5^+\|SiH^+\|COH^+$	$C_2H_5^+\|SiH^+\|COH^+$
30	$C_2H_6^+\|SiH_2^+\|COH_2^+$	–
31	$SiH_3^+\|COH_3^+$	$SiH_3^+\|COH_3^+$
39	$C_3H_3^+$	$C_3H_3^+$
41	$C_3H_5^+\|\ C_2OH^+$	$C_3H_5^+\|C_2OH^+$
42	$C_3H_6^+\|\ C_2OH_2^+\|CH_2Si^+$	–
43	$C_3H_7^+\|CH_3Si^+\|C_2OH_3^+$	$C_3H_7^+\|CH_3Si^+\|C_2OH_3^+$
45	$SiOH^+\|C_2H_6O^+$	–
50	$C_4H_2^+$	$C_4H_2^+$
51	–	$C_4H_3^+$
53	$C_4H_5^+\|C_3OH^+$	$C_4H_5^+\|C_3OH^+$
55	$C_2H_3Si^+\|C_4H_7^+\|C_3H_3O^+$	$C_2H_3Si^+\|C_4H_7^+\|C_3H_3O^+$
57	$C_3H_5O^+\|C_2H_5Si^+$	$C_3H_5O^+\|\ C_2H_5Si^+$
58	$C_2H_6Si^+\|C_3H_6O^+$	–
59	$C_2H_7Si^+\|C_3H_7O^+$	–
69	$C_4H_5O^+\|C_5H_9^+$	$C_4H_5O^+\|C_5H_9^+$
73	$C_3H_9Si^+$	–
93	$C_6H_5O^+\|C_7H_9^+$	$C_6H_5O^+\|C_7H_9^+$
97	$C_7H_{13}^+\|C_6H_9O^+$	–
100	$C_8H_4^+\|C_7O^+$	$C_8H_4^+\|C_7O^+$
119	$Si_2O(CH_3)_3(H)_2^+$	–
132	$Si_2O(CH_3)_4^+$	$Si_2O(CH_3)_4^+$
151	$Si_2O(CH_3)_5H_3^+$	–

(290 eV) and the O *K*-edge (530 eV), respectively. This means that two different sites are contributing to the fragmentation and desorption of these species and can be interpreted in terms of the ASID (Auger stimulated ion desorption) mechanism.[23,30] Similar behavior is observed for silicon ionic fragments (Si^+ and $SiCH_3^+$) in Figure 3. Here the electron energy is far away from the Si *K* (1 800 eV), Si L_I (150 eV), and $L_{II,III}$ (100 eV) edges, and the fragmentation mechanism leading to these species may be caused by a combination of carbon and oxygen 1s excitation/ionization processes.

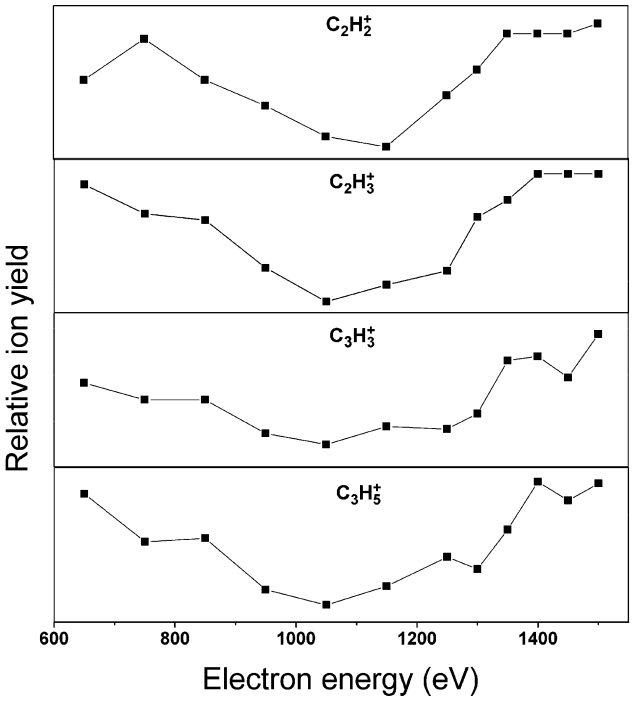

Figure 2. Relative desorption ion yield curves for $C_mH_n^+$ ions for HMDSO_1 sample as a function of electron energy.

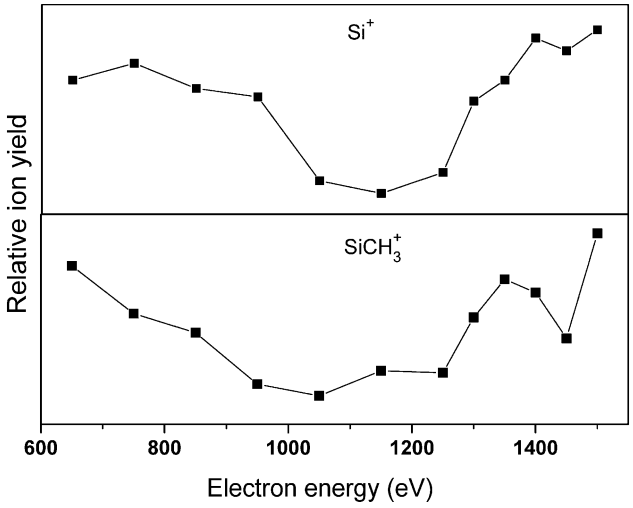

Figure 3. Relative desorption ion yield curves for Si^+ and $SiCH_3^+$ silicon ionic species for HMDSO_1 sample as a function of electron energy.

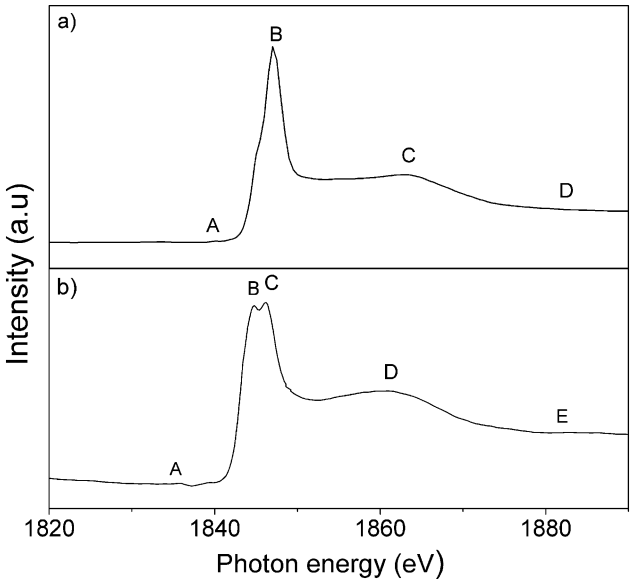

Figure 4. TEY NEXAFS spectra at the Si *K*-edge for (a) HDMSO_1 and (b) HDMSO_2 films.

3.2. NEXAFS and PSID Analysis

Figure 4 shows the photoabsorption (NEXAFS – Near-edge X-ray absorption fine structure) spectra of HDMSO_1 and HDMSO_2 films recorded at the silicon *K*-edge, covering from 1 820 to 1 890 eV photon energy. The HMDSO_1 NEXAFS spectrum is characterized by one (marked as **B** in Figure 4a) intense and narrow peak at 1 847 eV, while the HMDSO_2 NEXAFS spectrum shows two peaks (**B** and **C** in Figure 4b) at 1 844.8 and 1 846 eV, respectively. Similar features were found by Sutherland et al.[35] by comparing SiO_2 and $Si(OCH_3)_4$ NEXAFS spectra. The narrow peak in the HMDSO_1 spectrum is in accordance with the $1s \rightarrow \sigma^*(Si{-}O)$ electronic transition found in SiO_2 type structure, while the two electronic transitions in the HMDSO_2 spectrum are associated to $1s \rightarrow \sigma^*(Si{-}O)$ and $1s \rightarrow \sigma^*(Si{-}C)$ electronic transitions, respectively, similar to those observed in $Si(OCH_3)_4$ structure. These results corroborate the inorganic and organic character of HMDSO_1 and HMDSO_2 films, respectively. After identifying the electronic transitions from the Si 1s electron to unoccupied molecular orbitals, the photon energy marked **B** in both spectra was selected for the PSID experiments.

Table 3. Mass assignment and suggested fragments measured by PSID-TOF.

TOF (ns)	*m/z*	Assignment
46	28	$C_2H_4^+$
85	1	H^+
189	70	$SiCH_2Si^+$
233	14	Si^{2+}/CH_2^+
247	2	H_2^+
265	73/119	$Si(CH_3)_3^+/Si_2(CH_3)_3O(H)_2^+$
286	15	CH_3^+
296	30	$SiH_2^+/C_2H_6^+$

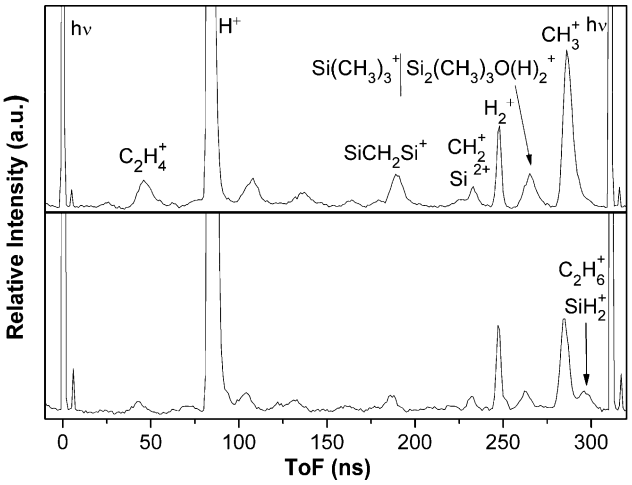

Figure 5. PSID spectra obtained at the Si *K*-edge for HMDSO_1 (top) and HMDSO_2 (bottom) films.

The assignment of the ionic fragments in PSID-TOF spectra (see Table 3) was performed using a similar procedure described for the ESID spectra analysis and the results are shown in Figure 5. For a comparative point of view these two PSID-TOF spectra were normalized with respect to the H^+ peak. Some differences are apparent. An accentuated decrease in the relative intensity for CH_3^+ species and the formation of a new peak localized at 296 a.m.u. corresponding to $SiH^+/C_2H_5^+$ ions was observed in the HMDSO_2 PSID spectrum. These results are in concordance with ESID results, where a reduction of CH_3^+ and an increase of the $SiH^+/C_2H_5^+$ species signal in the HMDSO_2 desorption spectrum was also measured.

4. Conclusion

In this work, plasma-polymerized HMDSO films were studied using ESID and PSID techniques. The organic–inorganic character of these polymers prepared by different processing routes was elucidated by ESID spectra and corroborated by PSID analysis. The presence of $SiOH^+$ and OH^+ species and higher masses of silicon ionic fragments in HMDSO_1 ESID spectrum are evidence of the inorganic character of this sample. In the case of HMDSO_2 polymer a high contribution of $C_2H_n^+$ species and the absence of higher mass fragments in the ESID spectrum are taken as a confirmation of the organic character of this sample. The ion

yield analysis for $C_nH_n^+$, Si^+ and $SiCH_3^+$ fragments in HMDSO_1 ESID spectra showed that these species are produced by Auger relaxation processes due to a combination of carbon and oxygen 1s ionizations. All other ionic fragments seem to be induced by indirect XESD relaxation processes. NEXAFS results showed one sharp feature in the silicon 1s absorption region for HMDSO_1 sample, evidencing that this film have SiO_2 inorganic structure, while the presence of two peaks for the HMDSO_2 film probes the existence of $Si(OCH_3)$ linked-edge and therefore the organic behavior. PSID results are in agreement with ESID analysis, where a decreasing of CH_3^+ species is observed for HMDSO_2 films, which was interpreted by the screening effect of the complex organic cross-linked structure in this polymer. These results show clearly the potentiality of the ESID and PSID techniques for the study of the chemical structure of plasma-polymerized films and to analyze surface modifications induced by different agents and processes.

Acknowledgements: Research partially supported by LNLS – National Synchrotron Light Laboratory, Brazil. The authors would like to thank CNPq, CAPES, and FAPERJ for financial support.

Received: January 15, 2013; Revised: February 18, 2013; Accepted: February 20, 2013; DOI: 10.1002/ppap.201300007

Keywords: electron stimulated ion desorption (ESID); hexamethyldisiloxane; photon stimulated ion desorption (PSID); plasma deposition; plasma-polymerization

[1] C. Rau, W. Kulisch, *Thin Solid Films* **1994**, *249*, 28.
[2] J. Schwartz, M. Schmidt, A. Ohl, *Surf. Coat. Technol.* **1998**, *98*, 859.
[3] M. Creatore, K. Kilic, A. O'Brien, K. Groenen, M. C. M. van de Sanden, *Thin Solid Films* **2003**, *427*, 137.
[4] J. Benedikt, D. Eijkman, W. Vandamme, S. Agarwal, M. C. M. Van de Sanden, *Chem. Phys. Lett.* **2005**, *402*, 37.
[5] A. M. Wróbel, M. R. Wertheimer, *In Plasma Deposition, Treatment and Etching of Polymers*, Academic Press, London **1991**, Chapter 3.
[6] A. M. Sarmadi, T. H. Ying, F. Denes, *Eur. Polym. J.* **1995**, *31*, 847.
[7] E. Schmachtenberg, F. R. Costa, S. Gobel, *J. Appl. Polym. Sci.* **2006**, *99*, 1485.
[8] Q. S. Yu, H. K. Yasuda, *J. Polym. Sci., Part A: Polym. Chem.* **1999**, *37*, 1577.
[9] L. Zuri, M. S. Silverstein, M. Narkis, *J. Appl. Polym. Sci.* **1996**, *62*, 2147.
[10] C. Vautrin-Ul, F. Roux, C. Boisse-Laporte, J. L. Pastol, A. Chausse, *J. Mater. Chem.* **2002**, *12*, 2318.
[11] M. J. Vasile, G. Smolinsky, *J. Electrochem. Soc.* **1972**, *119*, 451.
[12] R. Schmittgens, E. Schultheiss, *Czech. J. Phys.* **2006**, *56*, 1045.
[13] R. Schmittgens, B. Meyer, F. Stahr, K. Schade, E. Schultheiss, *Plasma Process. Polym.* **2007**, *4*, 5831.
[14] J. L. Jauberteau, L. Jauberteau, *J. Phys. Chem. A* **2012**, *116*, 8840.
[15] R. Morent, N. De Geyter, S. Van Vlierberghe, P. Dubruel, C. Leys, E. Schacht, *Surf. Coat. Technol.* **2009**, *203*, 1366.
[16] M. R. Alexander, F. R. Jones, R. D. Short, *Plasma. Polym.* **1997**, *2*, 277.
[17] R. Basner, R. Foest, M. Schmidt, K. Becker, H. Deutsch, *Int. J. Mass Spectrom. Ion. Process.* **1998**, *176*, 245.
[18] M. Creatore, Y. Barrell, J. Benedikt, M. C. M. van de Sander, *Plasma Sources Sci. Technol.* **2006**, *15*, 421.
[19] S. Carles, J. L. Le Garrec, J. B. Mitchell, *J. Chem. Phys.* **2007**, *127*, 144308.
[20] G. Araújo, C. Arantes, L. S. Roman, A. J. G. Zarbin, M. L. M. Rocco, *Surf. Sci.* **2009**, *603*, 647.
[21] D. E. Weibel, M. L. M. Rocco, F. C. Pontes, M. Ferreira, G. G. B. de Souza, *Polym. Degrad. Stab.* **2006**, *91*, 712.
[22] C. Arantes, A. M. Rocco, M. L. M. Rocco, *J. Electron Spectrosc. Relat. Phenom.* **2007**, *155*, 136.
[23] C. Arantes, A. M. Rocco, M. L. M. Rocco, *J. Electron Spectrosc. Relat. Phenom.* **2009**, *175*, 66.
[24] M. L. Knotek, *Rep. Prog. Phys.* **1984**, *47*, 1499.
[25] D. A. Dahl, SIMION 3D Version 6.0 User's Manual 1995.
[26] M. C. Corrêa, H. Tolentino, A. Craievich, C. Cusatis, *Rev. Sci. Instrum.* **1992**, *63*, 896.
[27] M. L. M. Rocco, G. S. Faraudo, F. C. Pontes, R. R. Pinho, M. Ferreira, G. G. B. de Souza, *Chem. Phys. Lett.* **2004**, *393*, 213.
[28] J. A. Bearden, A. F. Burr, *Rev. Mod. Phys.* **1967**, *39*, 125.
[29] M. L. M. Rocco, D. E. Weibel, F. C. Pontes, R. R. Pinho, G. S. Faraudo, G. G. B. de Souza, *Polym. Degrad. Stab.* **2003**, *80*, 263.
[30] L. A. V. Mendes, S. D. Magalhães, C. Arantes, M. L. M. Rocco, *Polym. Degrad. Stab.* **2007**, *92*, 741.
[31] P. N. Brookes, S. Fraser, R. D. Short, L. Hanley, E. Fuoco, A. Roberts, H. Hutton, *J. Electron Spectrosc. Relat. Phenom.* **2001**, *121*, 281.
[32] M. F. Piras, R. Di Mundo, F. Fracassi, A. Magnani, *Surf. Coat. Technol.* **2008**, *202*, 1606.
[33] M. R. Alexander, F. R. Jones, R. D. Short, *J. Phys. Chem. B* **1997**, *101*, 3614.
[34] C. Q. Jiao, C. A. DeJoseph, A. Garscadden, *J. Vac. Sci. Technol. A* **2005**, *23*, 1295.
[35] D. G. J. Sutherland, M. Kasrai, G. M. Bancrof, Z. F. Liu, K. H. Tan, *Phys. Rev. B* **1993**, *48*, 14989.